Published in final edited form as:
J Comp Neurol. 2008 September 20; 510(3): 297–308. doi:10.1002/cne.21788.

Connections and synaptic function in the posteroventral cochlear nucleus of deaf *jerker* mice

Xiao-Jie Cao[1], **Matthew J. McGinley**[2], and **Donata Oertel**[1]

[1] Department of Physiology, University of Wisconsin School of Medicine and Public Health, Madison, Wisconsin 53706

[2] Neuroscience Graduate Program, Vollum Institute, Oregon Health & Science University, Portland, Oregon 97239

Abstract

Mutations in the gene that encodes espins can cause deafness and vestibular disorders; mice that are homozygous for the autosomal recessive, *jerker* mutation in the espin gene never hear. Extracellular injections of biocytin into the anteroventral cochlear nucleus (AVCN) revealed that although the cochlear nuclei are smaller in *je*/*je* mice, the topography in its innervation resembles that in wild type mice. Auditory nerve fibers innervate narrow, topographically organized, "isofrequency" bands in deaf animals over the ages examined, P18–P70. The projection of tuberculoventral cells was topographic in *je*/*je* as in wild type mice. Terminals of auditory nerve fibers in the multipolar cell area included both large and small endings whereas in the octopus cell area they were exclusively small boutons in *je*/*je* as in wild type mice but end bulbs near the nerve root of *je*/*je* animals were smaller than in hearing animals. In whole-cell recordings from targets of auditory nerve fibers, octopus and T stellate cells, miniature excitatory postsynaptic currents (mEPSCs) had similar shapes as in +/+, indicating that the properties of AMPA receptors were not affected by the mutation. In *je*/*je* animals the frequency of spontaneous mEPSCs was elevated and synaptic depression in responses to trains of shocks delivered at between 100 and 333 Hz was greater than in wild type mice indicating that the probability of neurotransmitter release was increased. The frequency of spontaneous mEPSCs and extent of synaptic depression were greater in octopus than in T stellate cells, in both wild type and *je*/*je* mice.

Keywords

brain stem; auditory pathway; auditory nerve; hearing impairment; espin

INTRODUCTION

A goal of research in hearing is to understand how hearing loss affects auditory pathways in the brain. To understand how altered patterns of acoustically driven activity in the auditory nerve affect the structure and function of their targets in the ventral cochlear nucleus, we have compared neuronal circuitry and synaptic function between a strain of deaf inbred mice and wild type hearing mice.

Mutations in the gene that encodes the espin proteins cause non-syndromic deafness and vestibular disorders in human beings (Naz et al., 2004; Donaudy et al., 2006). The *Espn* gene encodes several isoforms of the actin-bundling protein, espin (Zheng et al., 2000). A

Send correspondence to: Donata Oertel, Department of Physiology, University of Wisconsin School of Medicine, 1300 University Ave, Madison, WI 53706, Phone: 608-263-6281, Fax: 608-265-5512, Email: oertel@physiology.wisc.edu.

spontaneous mutation in this gene in *jerker (je/je)* mice causes deafness as well as circling and head-shaking in homozygotes (Grueneberg et al., 1941; Deol, 1954; Steel and Bock, 1983). Homozygous *je*/*je* mice initially have a normal number of hair cells but these begin to degenerate rapidly starting at 11 days after birth. No cochlear microphonic potentials were recorded at any age (Steel and Bock, 1983).

We have examined how the *jerker* mutation affects the structure of the cochlear nuclei. The cochlear nuclei have long been known to be tonotopically organized as a consequence of their topographic innervation by auditory nerve fibers (Osen, 1970; Leake and Snyder, 1989). Connections between the dorsal and ventral cochlear nuclei, too, are bidirectional and topographically precise. Tuberculoventral neurons in the deep layer of the dorsal cochlear nucleus (DCN) inhibit regions of the ventral cochlear nucleus (VCN) that are innervated by the same auditory nerve fibers (Wickesberg and Oertel, 1988, 1990; Zhang and Oertel, 1993) (Fig. 1A). T Stellate cells in the VCN excite isofrequency bands in the deep layer of the DCN (Oertel et al., 1990; Doucet and Ryugo, 1997). The present experiments show that the topographic innervation pattern is precise even in animals that never hear.

Our electrophysiological studies focus on the function of two groups of principal cells in the posteroventral cochlear nucleus (PVCN) that lie adjacent to one another but have contrasting patterns of innervation, octopus and T stellate cells. These cells types also have contrasting projection patterns. Octopus cells project to the contralateral superior paraolivary nucleus and to the ventral nucleus of the lateral lemniscus (Adams and Warr, 1976; Warr, 1969; Schofield, 1995) whereas T stellate cells project to the contralateral inferior colliculus with collateral branches innervating the ventral nucleus of the trapezoid body and the ventral nucleus of the lateral lemniscus (Adams and Warr, 1976; Ryugo et al., 1981; Smith et al., 1993). The cells can be identified on the basis of their responses to current pulses; current pulses drive trains of action potentials in T stellate cells but evoke only a single action potential in octopus cells (Oertel et al., 1990; Golding et al., 1995; Golding et al., 1999; Bal and Oertel, 2000; Oertel et al., 2000; Bal and Oertel, 2001; Fujino and Oertel, 2001; Ferragamo and Oertel, 2002). The major excitatory input to each of these cell types comes from the auditory nerve. Each octopus cell is contacted by numerous (>60) auditory nerve fibers and requires the summation of input from more than about ten auditory nerve fibers to fire (Osen, 1969; Willott and Bross, 1990; Golding et al., 1995). In contrast, each T stellate cell receives input from only a few (5 to 6) auditory nerve fibers (Ferragamo et al., 1998). Not all excitation to these cells arises from auditory nerve fibers, however. Octopus cells receive excitatory input from other octopus cells (Golding et al., 1995) and T stellate cells receive excitatory input from other T stellate cells (Oertel et al., 1990; Ferragamo et al., 1998). Like all principal cells of the ventral cochlear nucleus, octopus and T stellate cells are excited through AMPA receptors with rapid channel-gating kinetics (Gardner et al., 1999; Gardner et al., 2001).

MATERIALS AND METHODS

Mice

Deaf *Espn*^{je} mice (JE/LeJ), also known as *jerker* mice and originally isolated as a spontaneous mutation, were obtained from the Jackson Labs. In hopes of developing a strain that breeds more easily, Dr. James Bartles at Northwestern University put the *Espn*^{je} allele into the CBA strain and generously supplied us with several breeding pairs of 10th generation heterozygotes. We detected no differences in the expression of the mutation on these two background strains. Experimental animals were obtained by breeding deaf *je*/*je* males with hearing *je*/+ females. We used the startle reflex to separate deaf, homozygous *je*/*je* mice from their hearing *je*/+ siblings. Initially wild type mice were inbred CBA mice from an in-house colony but after the colony succumbed to mouse hepatitis virus we routinely

ordered outbred ICR mice from Harlan Sprague Dawley. We have detected no differences in either the anatomy or physiology between CBA and ICR mice in the cochlear nuclei in our experiments over the 15 years that we have used these two strains. Biocytin injections were made into tissue from animals that ranged in age from 18 to 70 days old; electrophysiological experiments were performed on mice between 17 and 22 days old. Deaf *je*/*je* and *je*/+ mice seemed to grow and develop more slowly than +/+ mice; electrophysiological measurements on homozygous and heterozygous *jerker* mice were therefore performed on slices from animals that were on average somewhat older (Table 1).

Solutions

The extracellular physiological saline contained (in mM): 130 NaCl, 3 KCl, 1.3 $MgSO_4$, 2.4 $CaCl_2$, 20 $NaHCO_3$, 3 HEPES, 10 glucose, and 1.2 KH_2PO_4, pH 7.3–7.4 when saturated with 95%O_2, 5%CO_2 (≈ 305 mOsm). Measurements of the kinetics of mEPSCs were made in the presence of 1 μM tetrodotoxin and 1 μM strychnine. To separate currents mediated through AMPA receptors from those mediated through NMDA receptors, 100 μM D (−)-2-amino-5-phosphonopentanoic acid (APV) was added and 1 nM strychnine were included in the bath to block any inhibitory conductances.

Recording pipettes were filled with a solution which consisted of (in mM): 90 Cs_2SO_4, 20 CsCl, 5 EGTA, 10 HEPES, 4 Mg-ATP, 0.3 GTP, 5 Na-phosphocreatine, and was adjusted to pH 7.3 with CsOH (≈ 296 mOsm). Evoked EPSCs were recorded with pipettes to which 5 mM QX314 was also added. The final holding potentials were corrected for a −10 mV junction potential.

Preparation of slices

Coronal slices containing the PVCN were prepared from mice between 18 and 22 postnatal days old according to a protocol that was approved by the Institutional Animal Care and Use Commitee. Dissections were made in normal physiological saline at between 24–27 °C saturated with 95%O_2, 5%CO_2. After decapitation, the auditory nerve was cut, the brain was removed from the skull, and a block of tissue was glued at the level of the inferior colliculi. Slices of 200 μm thickness were cut using a vibrating microtome (Leica VT 1000S) and were then transferred to the recording chamber (~0.6 ml) and superfused continually at 5–6 ml/min with saline that was kept at 33°C by a custom-built, feedback-controlled heater.

Electrophysiological recordings

Whole-cell patch-clamp recordings were made using an Axopatch 200A amplifier (Axon instruments). Patch electrodes were made from borosilicate glass whose resistances ranged between 3.8–6 MΩ. All recordings of evoked and spontaneous EPSCs were digitized at 40 kHz and low-pass filtered at 10 kHz. The series resistance in 44 recordings, 11.1 ± 3.6 Mu, was compensated by 90–95% in recordings from octopus cells and by 70–75% in recordings from T-stellate cells with a 10 μsec lag. EPSCs were evoked by shocks through a Master-8 stimulator and Iso-flex isolator (AMPI, Jerusalem, Israel) of 100 μsec in duration and between 15 and 50 V amplitude, delivered through an extracellular-saline-filled glass pipette (~5 μm tip).

Data Analysis and Curve Fitting

Analysis of EPSCs was performed using pClamp (Clampfit 9.0, Axon Instruments). Exponential fits, amplitude, 10–90% rise time, decay time constant were measured off-line with pClamp software and a custom-designed current analysis program (Payne Chang, University of Wisconsin, Madison). The effects of genotype and cell type on properties of

EPSCs were evaluated using two-way ANOVA followed by Tukey's post test. All statistical tests were performed in Origin version 8.0 software. All values are given as means ± SE.

Anatomy

Anatomical studies to assess the circuitry were conducted as in an earlier study (Wickesberg and Oertel, 1988). With a single, parasagittal cut the cochlear nuclei were removed from the brain stem in a single "slice" that was 380 μm at its thickest point. The slice was maintained *in vitro* as in electrophysiological experiments. With a Picospritzer, saline containing 1% biocytin (Sigma) was injected into the AVCN through a pipette whose tip had a diameter of about 5 μm. Movement of the pipette through the slice disrupted fibers that crossed the injection site as pulses of pressure released biocytin. Biocytin was allowed to spread through the tissue for 1.5 to 2 hours as slices continued to be superfused with warmed, oxygenated saline. Slices were then fixed in 4% paraformaldahyde, stored at 4°C, embedded in a gelatin-albumin mixture, and resectioned at 40 to 60 μm with a vibratome. Biocytin in cells and fibers was visualized with horseradish peroxidase (Vectastain ABC Elite Kit, Vector Laboratories) (Golding et al., 1995). Photomicrographs were taken through a Zeiss Axioskop with a Zeiss Axiocam. Images were cropped and resized and the color was adjusted to compensate for the tungsten light source with Adobe Photoshop.

RESULTS

Topographic Organization

The cochlear nuclei receive a topographic projection from the cochlea through the auditory nerve that imposes a tonotopic organization on both the ventral and dorsal subdivisions. Bidirectional interconnections between the ventral and dorsal cochlear nuclei are also topographic. To assess whether the topographic organization of the cochlear nuclei was affected by deafness, biocytin was injected into the AVCN. Injections were made in slices of 6 *je*/*je* mice, 5 *je*/+ mice, 8 +/+ ICR, and 3 +/+ CBA mice between P18 and P27. In addition similar biocytin injections were made in 3 *je*/*je* and 1 *je*/+ mice between 66 and 70 days old. Although the cochlear nuclei of *je*/*je* mice even at three weeks of age were smaller than those of wild type mice, their organization was not obviously different (Fig. 1). As in the wild type, biocytin injections labeled topographically organized groups of fibers and neurons (Wickesberg and Oertel, 1988). They labeled a bundle of auditory nerve fibers that passed through the injection site so that fibers could be followed retrogradely to the nerve root and anterogradely through the multipolar cell area (mca) and octopus cell area (oca) of the PVCN to where they made a turn into the deep layer of the DCN. Some of the labeled terminals in the DCN are likely to have arisen from T stellate cells, whose axons follow the same path as the tuberculoventral cells (Wickesberg and Oertel, 1988;Oertel et al., 1990;Zhang and Oertel, 1993;Doucet and Ryugo, 1997). Within the band of labeled fibers and terminals in the DCN, labeled tuberculoventral neurons were evident (Fig. 1,B–E). There was no detectable difference between homozygous, heterozygous and wild type animals that were described previously (Wickesberg and Oertel, 1988). In each strain the terminals were localized to a band in the deep layer of the DCN that was roughly as wide as the 75 μm bands of terminals from individual T stellate cells (Oertel et al., 1990). A few cells were labeled ventral to the band of labeled terminals; the axon of these cells presumably passed through the injection site to innervate more ventral regions of the AVCN. The injections also labeled a group of neurons in the AVCN dorsal to the injection site (Fig. 1B, C), that are probably D stellate cells, whose dendrites and terminals can spread for large distances rostrocaudally as well as dorsoventrally (Wickesberg and Oertel, 1988;Oertel et al., 1990). The band of labeled neurons that lies within the band of labeled fibers in the AVCN likely includes T stellate cells whose dendrites spread along

isofrequency laminae (Oertel et al., 1990). In these tissues we also compared the morphology of the auditory nerve and its terminals between the wild type and *je*/*je* strains.

Auditory Nerve

The bundle of labeled auditory nerve axons could be followed back toward the nerve root, through the multipolar and octopus cell areas, and into the deep layer of the DCN. Multipolar and octopus cell areas were identified by the Nissl-staining pattern of the cell bodies. In mice, as in other mammalian species, multipolar cells are medium-sized and round with cytoplasm that stains unevenly whereas octopus cells are large and oval with cytoplasm that is homogeneous in its Nissl staining (Osen, 1969; Willard and Ryugo, 1983). Octopus cells lie posterior and medial to multipolar cells (Fig. 1B,C).

The terminals of auditory nerve fibers differ between regions of the ventral cochlear nucleus. Figure 2 shows that there was no gross difference in the morphology of auditory nerve terminations between strains. In each strain, auditory nerve fibers bifurcate in the nerve root (Fig. 2, nr, *) where end bulbs are common (Fig. 2, nr, eb). In the multipolar cell area, auditory nerve fibers terminate with small as well as large terminals (Fig. 2, mca, lt). Further dorsally, where auditory nerve fibers pass through the octopus cell area, terminals are exclusively small boutons (Fig. 2, oca). The *je*/*je* mouse whose auditory nerve terminals are illustrated in Figure 2 was 70 days old, showing also that there was no obvious difference in the innervation pattern between three-week old and 10-week old mice. Only in the shapes of end bulbs was there a subtle difference (Fig. 3). The end bulbs of deaf *je*/*je* mice tended to be smaller (Fig. 3A) than those in heterozygotes and wild type animals (Fig. 3B, C).

Identification of octopus and T stellate cells

The normal appearance of auditory nerve fibers in deaf *jerker* animals raised the question whether their function, too, is normal. We focused our studies on the physiological properties of synaptic inputs to multipolar and octopus cells because these cell types can be identified unambiguously. Octopus and T stellate cells are electrophysiologically distinct (Oertel et al., 1990; Ferragamo et al., 1998; Fujino and Oertel, 2001). Bushy cells are variable in their biophysical properties and could comprise two or three subpopulations even in wild type mice, making comparisons between wild type and *jerker* animals tricky (Cao et al., 2007). Responses to current pulses are illustrated in Figure 4. The strong hyperpolarization-activated mixed cation conductance (g_h) and strong low-voltage-activated K^+ conductance (g_{KL}) give octopus cells a low input resistance and prevent their firing repetitively. Even large currents evoke only a single action potential at the onset of a depolarization (Fig. 4A). In T stellate cells, on the other hand, even small currents evoke trains of action potentials whose undershoots rise monotonically back to rest (Fig. 4C).

To determine whether the properties of neurons are altered in deaf, *je*/*je* mice, we compared resting potentials, input resistances and membrane time constants near the resting potential. There were no significant differences in any of these parameters between wild type and *je*/*je* mice (Table 2).

Frequency of spontaneous mEPSCs is elevated in deaf je/je mice

The frequency of spontaneous mEPSCs reflects the properties of presynaptic terminals whereas their shape reflects the number and kinetics of the receptors that detect spontaneous release of neurotransmitter (Gardner et al., 1999). Spontaneous mEPSCs were recorded at −65 mV in the presence of 1 μM TTX and 1 μM strychnine (Fig. 4B, D). These mEPSCs were mediated through AMPA receptors because they were abolished by 20 μM DNQX. mEPSCs occurred more frequently in octopus and T-stellate cells from *je*/*je* than in those

from *je*/+ or +/+ mice ($F(2,41) = 14.9$, $p < 0.00002$; *je*/*je* vs. *je*/+, $p < 0.002$; *je*/*je* vs.+/+, $p < 0.0002$; *je*/+ vs. +/+, $p = 0.79$) (Fig. 5) . In octopus cells, the frequency of spontaneous mEPSCs in *je*/*je* mice was 82 ± 7 Hz (n=7) compared to 51 ± 8 Hz (n=5) in *je*/+ mice and 47 ± 5 Hz in +/+ mice (n=5) (Fig. 5). In T-stellate cells the frequency of mEPSCs was clearly lower than in octopus cells ($p < 10^{-7}$) but also significantly higher in *je*/*je* mice than in heterozygotes or wild type controls. In *je*/*je* mice mEPSCs in stellate cells occurred at 8 ± 0.6 Hz (n=10) whereas in *je*/+ mice they occurred at 3 ± 0.6 Hz (n=7) and in +/+ at 2 ± 0.5 Hz (n=8). There was a statistically significant interaction between the effects of genotype and cell type on the frequency of mEPSCs ($F(2,41) = 7.2$, $p < .005$).

There were no significant differences between mutant and wild type in the shapes of mEPSCs. Two-way ANOVA for measurements of amplitude, rise time and decay time constant in T stellate and octopus cells showed no effect of genotype ($F(2,41) = 0.06$, $p = 0.94$; $F(2,41) = 0.86$, $p = 0.43$; $F(2,41) = 1.6$, $p = 0.21$) (Fig. 5). In contrast, small differences in the shapes of mEPSCs between cell types were observed, as has been observed before (Gardner et al. 1999). The amplitude of mEPSCs was about 90 pA in T stellate cells and somewhat smaller, about 70 pA, in octopus cells ($p < 10^{-6}$). Despite the smaller amplitude, the 10–90% rise time of EPSCs in octopus cells, about 0.25 msec, was slightly longer than those in T stellate cells, which were about 0.18 msec ($p < 5.0 \times 10^{-6}$), possibly indicative ofmore dendritic filtering in octopus than in T stellate cells. The time constants, τ, of single exponential fits to the decay of mEPSCs were about 0.3 msec in both cell types ($p = 0.18$).

Synaptic depression is enhanced in je/je mice

We observed a difference in the robustness of synaptic responses not only between *je*/*je* and +/+ controls but also between octopus and T stellate cells (Fig. 6). Stimulation of bundles of fibers in the vicinity of the recorded neuron, presumably including either or both auditory nerve fibers and axons of excitatory interneurons, evoked inward currents in octopus and T-stellate neurons. The shock strength was adjusted to evoke EPSCs of about 1 nA at −65 mV (Fig. 6A). Responses to successive shocks that were delivered in trains at 100 Hz became progressively smaller. In wild type octopus cells, the amplitude of the 8th response was about 50% the amplitude of the 1st. In wild type T stellate cells there was only about 20% decrement in amplitude between the 1st and 8th responses (Fig. 6A). In *je*/*je* mice, depression was enhanced both in octopus and T stellate cells (Fig. 6B, C). In octopus cells the 8th response fell on average to 10% of the 1st response in *je*/*je* mice compared with 50% in wild type mice. In T stellate cells, the 8th response fell on average to 40% of the 1st compared with 80% in the wild type. Depression at auditory synapses depends on the maturity of tissue (Brenowitz and Trussell, 2001;Taschenberger and von Gersdorff, 2000). In the present experiments, the stronger depression in *je*/*je* mice could not have arisen from differences in age because measurements in homozygous and heterozygous jerker mice were generally made from older animals (Table 1).

Synaptic responses to trains of shocks at higher rates showed more depression but the patterns were similar (Fig. 7). Depression remained greater in octopus than in T stellate cells at all rates of stimulation. Depression was greater in *je*/*je* mice than in +/+ mice in both octopus and T stellate cells.

Evoked EPSCs in octopus and T stellate cells reflect input from multiple fibers. Responses in wild type octopus cells reflect a subset of inputs from >60 auditory nerve fibers and from an unknown number of octopus cells (Golding et al., 1995); responses in wild type T stellate cells reflect a subset of inputs from 5 or 6 auditory nerve fibers and an unknown number of inputs from other T stellate cells (Ferragamo et al., 1998). We cannot completely eliminate the possibility that conduction block develops at some fine branches when they are driven

repetitively but it seems more likely that the decrement in evoked EPSCs reflects synaptic function.

DISCUSSION

Animal models of deafness have provided important insights to understanding deafness and to understanding how the brain responds to the removal of synaptic inputs. The comparison of deaf *je*/*je* with hearing *je*/+ or +/+ mice revealed both surprising similarities and differences. Taken together, our results support the interpretation that spontaneous activity, together with developmental gradients, drive the development of orderly synaptic connections and that synapses in the PVCN increase their release probability in response to lack of acoustically driven input.

There were many similarities between deaf and hearing animals. First, although auditory nerve fibers are never driven acoustically, the cochlear nuclei were topographically sharply organized in *je*/*je* animals. Auditory nerve fibers and T stellate cells innervate a narrow, “isofrequency” band in the ventral and dorsal cochlear nuclei of *je*/*je* as in hearing mice. Those isofrequency bands in the DCN were roughly 100 μm wide, not much wider than the 75 μm bands of terminals of individual T stellate cells (Oertel et al., 1990). The topographically organized tuberculoventral projection from the deep layer of the DCN to the VCN was not noticeably different in deaf mutant and in hearing animals. Second, the morphology of terminals of auditory nerve fibers in the multipolar and octopus cell areas was not obviously different in *je*/*je* mice. In the multipolar cell area we observed both large and small terminals and in the octopus cell area only small boutons in deaf *je*/*je* mutant animals as in hearing animals. Third, the shapes of mEPSCs were similar in octopus and T stellate cells of all strains. Fourth, in wild type animals, synaptic responses to trains of shocks to the inputs showed more depression in octopus than in T stellate cells. Fifth, the intrinsic electrical properties of octopus and T stellate cells were not measurably different in deaf and hearing, three-week-old animals.

There were also differences between *je*/*je* and normally hearing *je*/+ and wild type mice. First, the end bulbs in the AVCN seemed to be smaller in *je*/*je* animals than in heterozygotes or control animals. Second, the frequency of spontaneous mEPSCs in both octopus and T stellate cells was greater in *je*/*je* animals than in *je*/+ or control mice. Third, synaptic depression was greater in *je*/*je* mice than in the wild type at all stimulation rates. The differences in mEPSC frequency and in synaptic depression suggest that terminals have a higher probability of neurotransmitter release in deaf *je*/*je* than in wild type mice (Zucker and Regehr, 2002).

The consequences of cochlear ablation have been studied in mammals and birds (reviewed by Harris and Rubel, 2006). Input through the auditory nerve influences profoundly the metabolism, survival and the patterns of connections among neurons of the auditory pathway. An important observation from cochlear ablation studies is that the consequences of deafferentation depend strongly upon age. When deafferentation occurs early in life within a critical period, it induces apoptotic death of target neurons whereas later in life deafferentation results in their shrinkage but loss of fewer of them. In the mouse the critical period lasts up to about P14 (Mostafapour et al., 2000). Neonatal cochlear ablation can result in abnormal patterns of synaptic connections (Kitzes et al., 1995).

Pre- and postsynaptic cells influence one another by means of electrical activity. Cochlear ablation thus leads to changes not only in cells that receive input directly from the auditory nerve but also at higher levels of the auditory pathway that are affected by changes in patterns and rates of synaptic activation (Powell and Erulkar, 1962; Smith et al., 1983; Sanes

and Takacs, 1993; Kotak and Sanes, 1997; Vale and Sanes, 2002; Sorensen and Rubel, 2006). Silencing the auditory nerve with tetrodotoxin after the critical period produces rapid changes and shrinkage of neurons in the VCN of gerbils and chicks (Pasic and Rubel, 1989; Pasic and Rubel, 1991). It has been shown repeatedly in sensory as well as motor systems that experience and synaptic activity guides the refinement of synaptic connections by eliminating some connections and strengthening others (Purves and Lichtman, 1980; Durham and Woolsey, 1985; Katz and Shatz, 1996; Knudsen, 1999). Pruning of connections is not universal, however; neuronal circuits in the olfactory system are elaborated with little sign of pruning (LaMantia and Purves, 1989; Pomeroy et al., 1990). It cannot be acoustically driven activity, but it could be spontaneous activity, that drives the organization of the topographic circuits in *je*/*je* mice. In rats it has recently been shown that groups of supporting cells in Kolliker's organ produce calcium waves that activate small groups of inner hair cells (Tritsch et al., 2007). The coactivation of auditory nerve fibers associated with the stimulation of small groups of inner hair cells could lead to the segregation of their terminals in sharp "isofrequency" laminae in the cochlear nuclei. Spontaneous activity has long been suspected to play a role in the development of the auditory system (Walsh and McGee, 1987; Lippe, 1994; McKay and Oleskevich, 2007). In slice cultures the development of topographic organization between the medial nucleus of the trapezoid body and the lateral superior olivary nucleus depends on electrical activity and synaptic input (Lohmann et al., 1998).

Genetic models of deafness are valuable because they resemble many forms of human deafness. As in *je*/*je* mice, human deafness often leaves auditory nerve fibers intact. In humans, as in mutant animals, hair cells are present before the onset of hearing and then degenerate but often a substantial proportion of auditory nerve fibers remain. Remaining auditory nerve fibers can be stimulated through implants in congenitally deaf white cats and enable them to use their auditory pathway (Hartmann et al., 1997; Heid et al., 1997). In these animals the end bulb endings of auditory nerve fibers that contact bushy cells in the AVCN are larger and more branched than their counterparts in hearing cats (Ryugo et al., 1997) but at higher levels of the auditory pathway changes were not detected (Heid et al., 1997).

Recently several detailed studies have been made of genetic models of deafness in mice. Ryugo and his colleagues have compared the morphology of end bulbs of Held in wild type with those in deaf *shaker* mice, mice with a recessive mutation in the gene that encodes myosin 15 (Limb and Ryugo, 2000). Walmsley and his colleagues have studied mice that carry an autosomal recessive mutation in the gene that encodes the transmembrane cochlear-expressed gene 1 (TMC1), the *deafness* gene. Like the *je*/*je* mice, *dn*/*dn* mice have hair cells early in life that degenerate and the mice never hear (Bock and Steel, 1980). Manis and his colleagues have examined mice of the DBA strain that lose high-frequency hearing even in the first month of life. This strain of inbred mice has multiple recessive mutations, including in *cadherin 23* (Cdh^{753A}), modifier of deafwaddler (*mdwd*), the mitochondrial mutation $mt\text{-}Tr^{9827ins8}$, and *Atp2b2* (Noben-Trauth et al., 2003). Together with the present study the comparisons are interesting for both the similarities and differences.

In three strains of deaf mice, as in cats, the end bulbs of Held differ morphologically from those of hearing mice. We show that in *jerker* mice between P20 and P70 end bulbs are smaller. Limb and Ryugo examined end bulbs over a range of ages and showed that end bulbs in *shaker* mice are not simply immature versions of normal end bulbs but have a different, less branched morphology than in hearing mice (Limb and Ryugo, 2000). In *dn*/*dn* mice at P20-P22 end bulbs are smaller than in control animals but calyceal terminals in the medial nucleus of the trapezoid body are unaltered (Youssoufian et al., 2008).

The properties of the synaptic connections between end bulbs and their bushy cell targets are affected differently in three mouse models of hearing impairment, cochlear ablation, *dn*/*dn* and DBA mice. Recordings from bushy and stellate cells in the AVCN of three-week-old mice, one week after cochlear ablation, showed that in stellate cells there were few changes but that in bushy cells spontaneous miniature EPSCs were more frequent and showed more dendritic filtering than in normal mice (Lu et al., 2007). In *dn*/*dn* mice, mEPSCs were larger and release probability was increased relative to those in hearing mice (Oleskevich and Walmsley, 2002; McKay and Oleskevich, 2007). In contrast, mEPSCs were smaller and less frequent in the dorsal regions of the AVCN that suffered hearing loss relative to those in the ventral regions in DBA mice (Wang and Manis, 2005). Bushy cells are of at least two distinct types, spherical that project to the lateral and medial superior olives and globular that project to the medial nucleus of the trapezoid body. They are also biophysically heterogeneous, making it difficult to distinguish differences within the population of bushy cells from differences between populations (McGinley and Oertel, 2006; Cao et al., 2007).

The properties of the synaptic connections between auditory nerve fibers and targets in the PVCN have not been examined in other mouse models of hearing impairment. The differences we have observed in the PVCN of *je*/*je* mice are unlike either of the patterns observed in the AVCN of *dn*/*dn* or DBA mice. We observed no changes in amplitude of spontaneous mEPSCs. The changes in frequency of mEPSCs were like those observed at end bulbs in *dn*/*dn* mice but unlike those in DBA mice.

The pattern of changes we observe, that there is an increase in the frequency but not in the amplitude of mEPSCs, differs from that observed in the AVCN of *dn*/*dn* and DBA mice and after cochlear ablation. Differences could result from differences in genetic defects. Although mutations in the espins cause non-syndromic deafness in humans, espins are expressed not only in the cochlea but also in auditory nerve terminals in the VCN (Sekerkova et al., 2007). We cannot therefore attribute differences between *je*/*je* and normally hearing mice to deafness with certainty; differences could possibly have resulted from a direct effect of the mutation on terminals. The multiple mutations associated with the DBA strain could also affect the function of neurons directly in addition to changing patterns of activity in the auditory nerve. The TMC1 protein that is altered by the *deafnes*s mutation is presumably expressed only in the cochlea. Another important variable is age; recordings from *dn*/*dn* mice were made at P9–12, in *je*/*je* mice they were made at ~P20, and in DBA mice they were made at up to P65. A third important variable is temperature; recordings in *je*/*je*, DBA, and mice with cochlear ablations were made at ~33°C, whereas those in *dn*/*dn* mice were made at ~22°C.

Whether hearing loss affects the intrinsic properties of neurons is an interesting question because it is possible that increases in intrinsic excitability could underly some forms of tinnitus. Octopus cells detect coincident firing in auditory nerve fibers that innervate them. In normally hearing animals, large populations of auditory nerve fibers are driven synchronously by broadband sounds. In the absence of hearing, in contrast, it seems unlikely that large populations of auditory nerve fibers fire synchronously (Tritsch et al., 2007). We tested whether octopus cells respond to altered firing patterns by increasing their input resistance but found no differences in the resting potential or input resistance of either octopus or T stellate cells between *je*/*je* and wild type mice. Increases in excitability that result from a reduction in low-voltage-activated K^+ conductances have been detected in the medial nucleus of the trapezoid body in *dn*/*dn* mice (Leao et al., 2004). In the dorsal AVCN that is subject to hearing loss, the excitability of presumed bushy cells decreased (Wang and Manis, 2006). Interpretation of these findings is complicated by the variability of properties among bushy cells; the input resistances measured by Wang and Manis even in CBA mice are higher than those we measured from the same strain of mice (Cao et al., 2007). Altered

activity has also been associated with changes in intrinsic electrical properties in hippocampal and cortical neurons (Fan et al., 2005; Kotak et al., 2005).

In both *je*/*je* and wild type mice, synaptic depression was more prominent in octopus than in T stellate cells. Auditory nerve fibers and octopus cells can be driven at rates that approach 1000 Hz *in vitro* (Oertel, 1983; Golding et al., 1995; Oertel et al., 2000). *In vivo*, too, octopus cells can be driven at very high rates (Rhode and Smith, 1986; Oertel et al., 2000). *In vivo* T stellate cells can also be driven at over 1000 Hz (Blackburn and Sachs, 1989). Knowing that these cells can be driven to fire so rapidly, it would seem unlikely that conduction block would occur when the firing rate is ten times slower. We conclude that the depression we observe is likely to be largely synaptic depression. We were surprised at how much synaptic depression was evident in octopus cells because earlier sharp-electrode recordings had suggested that these neurons fire robustly even in responses to shocks at >300 Hz (Golding et al., 1995). This difference may in part result from a difference in age of the animals. In the present study slices were from animals at P17 – P22 whereas one third of animals in the earlier study were from animals at P23 – P26; maturation is known to affect synapses in the auditory system (Taschenberger and von Gersdorff, 2000; Brenowitz and Trussell, 2001). Consistent with the present results, earlier sharp-electrode recordings from T stellate cells reveal little depression (Wu and Oertel, 1987).

It has been observed before that short-term plasticity varies among terminals of a single neuron (Reyes et al., 1998; Rozov et al., 2001). In the cochlear nuclei of birds short-term plasticity has been shown to vary among targets of auditory nerve fibers; depression is more prominent in nucleus magnocellularis, whose neurons encode timing, and facilitation is more prominent in nucleus angularis where at least some neurons encode intensity (MacLeod et al., 2007). MacLeod and colleagues point out that with less depression, neurons transmit rate of firing of auditory nerve fibers more linearly; in transmitting firing rate, such synapses are well suited to encode intensity. This observation is consistent with what is known about T stellate cells in mammals. Several observations indicate that as a population T stellate cells (choppers) encode the spectrum of sounds (Blackburn and Sachs, 1989; Fujino and Oertel, 2001; Young and Sachs, 2008).

Acknowledgments

We received much help in this project for which we are grateful indeed. We are especially grateful to James Bartles for sharing his preliminary results and for supplying us with mice. John H. Wittig Jr. helped us to identify technical problems that were then rectified, Inge Siggelkow processed tissues histologically, Ravi Kochhar kept our computers humming, the staff of the department of Physiology keep papers moving in appropriate directions, and Bryan Seybold and Samantha Wright read the manuscript critically. This work was supported by a grant from the NIH DC 00176.

LITERATURE CITED

Adams JC, Warr WB. Origins of axons in the cat's acoustic striae determined by injection of horseradish peroxidase into severed tracts. J Comp Neurol. 1976; 170:107–121. [PubMed: 61976]

Bal R, Oertel D. Hyperpolarization-activated, mixed-cation current (Ih) in octopus cells of the mammalian cochlear nucleus. J Neurophysiol. 2000; 84:806–817. [PubMed: 10938307]

Bal R, Oertel D. Potassium currents in octopus cells of the mammalian cochlear nuclei. J Neurophysiol. 2001; 86:2299–2311. [PubMed: 11698520]

Blackburn CC, Sachs MB. Classification of unit types in the anteroventral cochlear nucleus: PST histograms and regularity analysis. J Neurophysiol. 1989; 62:1303–1329. [PubMed: 2600627]

Bock GR, Steel K. Cochlear potentials in deafness and jerker mice. J Acoust Soc Am. 1980; 67(Suppl 1):S89.

Brenowitz S, Trussell LO. Maturation of synaptic transmission at end-bulb synapses of the cochlear nucleus. J Neurosci. 2001; 21:9487–9498. [PubMed: 11717383]

Cao XJ, Shatadal S, Oertel D. Voltage-sensitive conductances of bushy cells of the mammalian ventral cochlear nucleus. J Neurophysiol. 2007; 97:3961–3975. [PubMed: 17428908]

Deol MS. The anomalies of the labyrinth of the mutants varitint-waddler, shaker-2 and jerker in the mouse. J Genet. 1954; 52:562–588.

Donaudy F, Zheng L, Ficarella R, Ballana E, Carella M, Melchionda S, Estivill X, Bartles JR, Gasparini P. Espin gene (ESPN) mutations associated with autosomal dominant hearing loss cause defects in microvillar elongation or organisation. J Med Genet. 2006; 43:157–161. [PubMed: 15930085]

Doucet JR, Ryugo DK. Projections from the ventral cochlear nucleus to the dorsal cochlear nucleus in rats. J Comp Neurol. 1997; 385:245–264. [PubMed: 9268126]

Durham D, Woolsey TA. Functional organization in cortical barrels of normal and vibrissae-damaged mice: a (3H) 2-deoxyglucose study. J Comp Neurol. 1985; 235:97–110. [PubMed: 2985659]

Fan Y, Fricker D, Brager DH, Chen X, Lu HC, Chitwood RA, Johnston D. Activity-dependent decrease of excitability in rat hippocampal neurons through increases in I(h). Nat Neurosci. 2005; 8:1542–1551. [PubMed: 16234810]

Ferragamo MJ, Golding NL, Oertel D. Synaptic inputs to stellate cells in the ventral cochlear nucleus. J Neurophysiol. 1998; 79:51–63. [PubMed: 9425176]

Ferragamo MJ, Oertel D. Octopus cells of the mammalian ventral cochlear nucleus sense the rate of depolarization. J Neurophysiol. 2002; 87:2262–2270. [PubMed: 11976365]

Fujino K, Oertel D. Cholinergic modulation of stellate cells in the mammalian ventral cochlear nucleus. J Neurosci. 2001; 21:7372–7383. [PubMed: 11549747]

Gardner SM, Trussell LO, Oertel D. Time course and permeation of synaptic AMPA receptors in cochlear nuclear neurons correlate with input. J Neurosci. 1999; 19:8721–8729. [PubMed: 10516291]

Gardner SM, Trussell LO, Oertel D. Correlation of AMPA receptor subunit composition with synaptic input in the mammalian cochlear nuclei. J Neurosci. 2001; 21:7428–7437. [PubMed: 11549753]

Golding NL, Ferragamo MJ, Oertel D. Role of intrinsic conductances underlying responses to transients in octopus cells of the cochlear nucleus. J Neurosci. 1999; 19:2897–2905. [PubMed: 10191307]

Golding NL, Robertson D, Oertel D. Recordings from slices indicate that octopus cells of the cochlear nucleus detect coincident firing of auditory nerve fibers with temporal precision. J Neurosci. 1995; 15:3138–3153. [PubMed: 7722652]

Grueneberg H, Burnett J, Snell GD. The origin of jerker, a new gene mutation of the house mouse, and linkage studies made with it. Proc Nat Acad Sci USA. 1941; 27:562–565. [PubMed: 16588504]

Harris JA, Rubel EW. Afferent regulation of neuron number in the cochlear nucleus: cellular and molecular analyses of a critical period. Hear Res. 2006; 216–217:127–137.

Hartmann R, Shepherd RK, Heid S, Klinke R. Response of the primary auditory cortex to electrical stimulation of the auditory nerve in the congenitally deaf white cat. Hear Res. 1997; 112:115–133. [PubMed: 9367234]

Heid S, Jahn-Siebert TK, Klinke R, Hartmann R, Langner G. Afferent projection patterns in the auditory brainstem in normal and congenitally deaf white cats. Hear Res. 1997; 110:191–199. [PubMed: 9282901]

Katz LC, Shatz CJ. Synaptic activity and the construction of cortical circuits. Science. 1996; 274:1133–1138. [PubMed: 8895456]

Kitzes LM, Kageyama GH, Semple MN, Kil J. Development of ectopic projections from the ventral cochlear nucleus to the superior olivary complex induced by neonatal ablation of the contralateral cochlea. J Comp Neurol. 1995; 353:341–363. [PubMed: 7751435]

Knudsen EI. Mechanisms of experience-dependent plasticity in the auditory localization pathway of the barn owl. J Comp Physiol [A]. 1999; 185:305–321.

Kotak VC, Fujisawa S, Lee FA, Karthikeyan O, Aoki C, Sanes DH. Hearing loss raises excitability in the auditory cortex. J Neurosci. 2005; 25:3908–3918. [PubMed: 15829643]

Kotak VC, Sanes DH. Deafferentation weakens excitatory synapses in the developing central auditory system. European J Neurosci. 1997; 9:2340–2347. [PubMed: 9464928]

LaMantia AS, Purves D. Development of glomerular pattern visualized in the olfactory bulbs of living mice. Nature. 1989; 341:646–649. [PubMed: 2797191]

Leake PA, Snyder RL. Topographic organization of the central projections of the spiral ganglion in cats. J Comp Neurol. 1989; 281:612–629. [PubMed: 2708585]

Leao RN, Berntson A, Forsythe ID, Walmsley B. Reduced low-voltage activated K+ conductances and enhanced central excitability in a congenitally deaf (dn/dn) mouse. J Physiol. 2004; 559:25–33. [PubMed: 15235085]

Limb CJ, Ryugo DK. Development of primary axosomatic endings in the anteroventral cochlear nucleus of mice. J Assoc Res Otolaryngol. 2000; 1:103–119. [PubMed: 11545139]

Lippe WR. Rhythmic spontaneous activity in the developing avian auditory system. J Neurosci. 1994; 14:1486–1495. [PubMed: 8126550]

Lohmann C, Ilic V, Friauf E. Development of a topographically organized auditory network in slice culture is calcium dependent. J Neurobiology. 1998; 34:97–112.

Lu Y, Harris JA, Rubel EW. Development of spontaneous miniature EPSCs in mouse AVCN neurons during a critical period of afferent-dependent neuron survival. J Neurophysiol. 2007; 97:635–646. [PubMed: 17079338]

MacLeod KM, Horiuchi TK, Carr CE. A role for short-term synaptic facilitation and depression in the processing of intensity information in the auditory brain stem. J Neurophysiol. 2007; 97:2863–2874. [PubMed: 17251365]

McGinley MJ, Oertel D. Rate thresholds determine the precision of temporal integration in principal cells of the ventral cochlear nucleus. Hear Res. 2006; 216–217:52–63.

McKay SM, Oleskevich S. The role of spontaneous activity in development of the endbulb of Held synapse. Hear Res. 2007; 230:53–63. [PubMed: 17590547]

Mostafapour SP, Cochran SL, Del Puerto NM, Rubel EW. Patterns of cell death in mouse anteroventral cochlear nucleus neurons after unilateral cochlea removal. J Comp Neurol. 2000; 426:561–571. [PubMed: 11027399]

Naz S, Griffith AJ, Riazuddin S, Hampton LL, Battey JF Jr, Khan SN, Riazuddin S, Wilcox ER, Friedman TB. Mutations of ESPN cause autosomal recessive deafness and vestibular dysfunction. J Med Genet. 2004; 41:591–595. [PubMed: 15286153]

Noben-Trauth K, Zheng QY, Johnson KR. Association of cadherin 23 with polygenic inheritance and genetic modification of sensorineural hearing loss. Nat Genet. 2003; 35:21–23. [PubMed: 12910270]

Oertel D. Synaptic responses and electrical properties of cells in brain slices of the mouse anteroventral cochlear nucleus. J Neurosci. 1983; 3:2043–2053. [PubMed: 6619923]

Oertel D, Bal R, Gardner SM, Smith PH, Joris PX. Detection of synchrony in the activity of auditory nerve fibers by octopus cells of the mammalian cochlear nucleus. Proc Nat Acad Sci USA. 2000; 97:11773–11779. [PubMed: 11050208]

Oertel D, Wu SH, Garb MW, Dizack C. Morphology and physiology of cells in slice preparations of the posteroventral cochlear nucleus of mice. J Comp Neurol. 1990; 295:136–154. [PubMed: 2341631]

Oleskevich S, Walmsley B. Synaptic transmission in the auditory brainstem of normal and congenitally deaf mice. J Physiol. 2002; 540:447–455. [PubMed: 11956335]

Osen KK. Cytoarchitecture of the cochlear nuclei in the cat. J Comp Neurol. 1969; 136:453–484. [PubMed: 5801446]

Osen KK. Course and termination of the primary afferents in the cochlear nuclei of the cat. Arch Ital Biol. 1970; 108:21–51. [PubMed: 5438720]

Pasic TR, Rubel EW. Rapid changes in cochlear nucleus cell size following blockade of auditory nerve electrical activity in gerbils. J Comp Neurol. 1989; 283:474–480. [PubMed: 2745750]

Pasic TR, Rubel EW. Cochlear nucleus cell size is regulated by auditory nerve electrical activity. Otolaryngol-Head-Neck-Surg. 1991; 104:6–13. [PubMed: 1900632]

Pomeroy SL, LaMantia AS, Purves D. Postnatal construction of neural circuitry in the mouse olfactory bulb. J Neurosci. 1990; 10:1952–1966. [PubMed: 2355260]

Powell TPS, Erulkar S. Transneuronal cell degeneration in the auditory relay nuclei of the cat. J Anat. 1962; 96:249–268. [PubMed: 14488390]

Purves D, Lichtman JW. Elimination of synapses in the developing nervous system. Science. 1980; 210:153–157. [PubMed: 7414326]

Reyes A, Lujan R, Rozov A, Burnashev N, Somogyi P, Sakmann B. Target-cell-specific facilitation and depression in neocortical circuits. Nat Neurosci. 1998; 1:279–285. [PubMed: 10195160]

Rhode WS, Smith PH. Encoding timing and intensity in the ventral cochlear nucleus of the cat. J Neurophysiol. 1986; 56:261–286. [PubMed: 3760921]

Rozov A, Burnashev N, Sakmann B, Neher E. Transmitter release modulation by intracellular Ca2+ buffers in facilitating and depressing nerve terminals of pyramidal cells in layer 2/3 of the rat neocortex indicates a target cell-specific difference in presynaptic calcium dynamics. J Physiol. 2001; 531:807–826. [PubMed: 11251060]

Ryugo DK, Pongstaporn T, Huchton DM, Niparko JK. Ultrastructural analysis of primary endings in deaf white cats: morphologic alterations in endbulbs of Held. J Comp Neurol. 1997; 385:230–244. [PubMed: 9268125]

Ryugo DK, Willard FH, Fekete DM. Differential afferent projections to the inferior colliculus from the cochlear nucleus in the albino mouse. Brain Res. 1981; 210:342–349. [PubMed: 6164444]

Sanes DH, Takacs C. Activity-dependent refinement of inhibitory connections. Eur J Neurosci. 1993; 5:570–574. [PubMed: 8261131]

Schofield BR. Projections from the cochlear nucleus to the superior paraolivary nucleus in guinea pigs. J Comp Neurol. 1995; 360:135–149. [PubMed: 7499559]

Sekerkova G, Zheng L, Mugnaini E, Bartles JR. Espin proteins are concentrated in the auditory nerve fibers innervating root neurons and octopus cells in the rat cochlear nucleus. Soc Neurosci Abstr. 2007; 67:12.

Smith, PH.; Joris, PX.; Banks, MI.; Yin, TCT. Responses of cochlear nucleus cells and projections of their axons. In: Merchan, MA.; Juiz, JM.; Godfrey, DA.; Mugnaini, E., editors. The Mammalian Cochlear Nuclei, Organization and Function. New York and London: Plenum Press; 1993. p. 349-360.

Smith ZD, Gray L, Rubel EW. Afferent influences on brainstem auditory nuclei of the chicken: n. laminaris dendritic length following monaural conductive hearing loss. J Comp Neurol. 1983; 220:199–205. [PubMed: 6315783]

Sorensen SA, Rubel EW. The level and integrity of synaptic input regulates dendrite structure. J Neurosci. 2006; 26:1539–1550. [PubMed: 16452677]

Steel KP, Bock GR. Cochlear dysfunction in the jerker mouse. Behav Neurosci. 1983; 97:381–391. [PubMed: 6871029]

Taschenberger H, von Gersdorff H. Fine-tuning an auditory synapse for speed and fidelity: developmental changes in presynaptic waveform, EPSC kinetics, and synaptic plasticity. J Neurosci. 2000; 20:9162–9173. [PubMed: 11124994]

Tritsch NX, Yi E, Gale JE, Glowatzki E, Bergles DE. The origin of spontaneous activity in the developing auditory system. Nature. 2007; 450:50–55. [PubMed: 17972875]

Vale C, Sanes DH. The effect of bilateral deafness on excitatory and inhibitory synaptic strength in the inferior colliculus. Eur J Neurosci. 2002; 16:2394–2404. [PubMed: 12492434]

Walsh EJ, McGee J. Postnatal development of auditory nerve and cochlear nucleus neuronal responses in kittens. Hear Res. 1987; 28:97–116. [PubMed: 3610862]

Wang Y, Manis PB. Synaptic transmission at the cochlear nucleus endbulb synapse during age-related hearing loss in mice. J Neurophysiol. 2005; 94:1814–1824. [PubMed: 15901757]

Wang Y, Manis PB. Temporal coding by cochlear nucleus bushy cells in DBA/2J mice with early onset hearing loss. J Assoc Res Otolaryngol. 2006; 7:412–424. [PubMed: 17066341]

Warr WB. Fiber degeneration following lesions in the posteroventral cochlear nucleus of the cat. Exp Neurol. 1969; 23:140–155. [PubMed: 5765002]

Wickesberg RE, Oertel D. Tonotopic projection from the dorsal to the anteroventral cochlear nucleus of mice. J Comp Neurol. 1988; 268:389–399. [PubMed: 3360996]

Wickesberg RE, Oertel D. Delayed, frequency-specific inhibition in the cochlear nuclei of mice: A mechanism for monaural echo suppression. J Neurosci. 1990; 10:1762–1768. [PubMed: 1972392]

Willard, FH.; Ryugo, DK. Anatomy of the central auditory system. In: Willott, JF., editor. The Auditory Psychobiology of the Mouse. Springfield: Charles C Thomas; 1983. p. 201-304.

Willott JF, Bross LS. Morphology of the octopus cell area of the cochlear nucleus in young and aging C57BL/6J and CBA/J mice. J Comp Neurol. 1990; 300:61–81. [PubMed: 2229488]

Wu SH, Oertel D. Maturation of synapses and electrical properties. Hearing Res. 1987; 30:99–110.

Young ED, Sachs M. Auditory nerve inputs to cochlear nucleus neurons studied with cross-correlation. Neurosci. 2008 in press.

Youssoufian M, Couchman K, Shivdasani MN, Paolini AG, Walmsley B. Maturation of auditory brainstem projections and calyces in the congenitally deaf (dn/dn) mouse. J Comp Neurol. 2008; 506:442–451. [PubMed: 18041784]

Zhang S, Oertel D. Tuberculoventral cells of the dorsal cochlear nucleus of mice: intracellular recordings in slices. J Neurophysiol. 1993; 69:1409–1421. [PubMed: 8389823]

Zheng L, Sekerkova G, Vranich K, Tilney LG, Mugnaini E, Bartles JR. The deaf jerker mouse has a mutation in the gene encoding the espin actin-bundling proteins of hair cell stereocilia and lacks espins. Cell. 2000; 102:377–385. [PubMed: 10975527]

Zucker RS, Regehr WG. Short-term synaptic plasticity. Ann Rev Physiol. 2002; 64:355–405. [PubMed: 11826273]

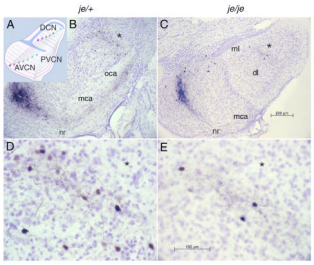

Figure 1.

Tonotopic organization of the cochlear nuclei is unaltered by the *jerker* mutation. A: A schematic representation of the topographic organization of the tuberculoventral cell projections from the dorsal (DCN) to the anteroventral (AVCN) and posteroventral cochlear nucleus (PVCN) that underlies the labeling pattern. A sheet of granule cells separates the ventral from the dorsal cochlear nucleus (blue); granule and other cell bodies separate the outer, molecular layer from the innermost deep layer (blue). Auditory nerve fibers impose a tonotopic organization on both the VCN and DCN; those fibers that encode the lowest frequencies (brown) terminate ventrally and those that encode the highest frequencies (blue-green) terminate dorsally. Tuberculoventral cells project to targets in the AVCN and PVCN that receive input from the same group of auditory nerve fibers and are therefore tuned to similar frequencies. (The topographic projection of T stellate cells to the DCN is not illustrated.) B: Photomicrograph of a parasagittal section of a slice of the cochlear nuclei from a heterozygous, *je*/+, normally hearing mouse in which an injection of biocytin had been made into the AVCN. The injection labeled a cluster of auditory nerve fibers that can be traced retrogradely from the injection site to the nerve root (nr) and anterogradely through the multipolar (mca) and octopus cell areas (oca) in the PVCN into the deep layer (dl), but not the molecular layer (ml), of the DCN. C: In a homozygous, deaf, *je*/*je* mouse the labeling pattern resembles that of the heterozygote. The oca is not present in this lateral section. D, E: Labeled fibers and cell bodies in the deep layer of the DCN in the same sections illustrated in B and C are shown at higher magnification, with asterisks (*) indicating corresponding points in panels B and D and in panels C and E. Within the bands of labeled fibers in the deep layer of the dorsal cochlear nucleus (DCN) lay bands of tuberculoventral cell bodies that were labeled through their terminals at the injection site. A few labeled cell bodies ventral to the band of labeled fibers were labeled through axons that passed through the injection site en route to more ventral regions of the AVCN.

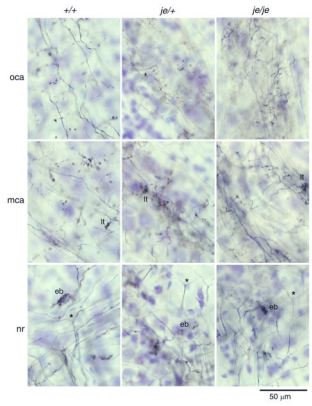

Figure 2.

Innervation of the PVCN by auditory nerve fibers is not obviously affected by the *jerker* mutation. Each column shows photomicrographs from a single animal: an outbred, ICR mouse 22 days old is depicted on the left, a heterozygote, *je*/+ mouse 24 days old is depicted in the middle, and a deaf homozygous *je*/*je* mouse 70 days old is depicted on the right. Rows of panels show labeled fibers in comparable locations, the nerve root (NR), more caudally and dorsally in the multipolar cell area (MCA), and in the most caudal and dorsal tip of the PVCN that contained large cell bodies of octopus cells (OCA). Auditory nerve fibers entered the brain stem at the nerve root where they bifurcated (*); one branch headed anteriorly to the AVCN and the other posteriorly to the PVCN. End bulbs (eb) were commonly observed near the nerve root. Throughout the PVCN, collateral fibers emanated from the main auditory nerve fiber and terminated. In the MCA some terminals were single boutons but larger terminals (lt) were also apparent. In the OCA, auditory nerve terminals were more uniform in size and comprised almost exclusively small boutons. There were no obvious differences in the morphology or pattern of termination between strains of mice. All photomicrographs are in the parasagittal plane and show anterior on the right and dorsal upward.

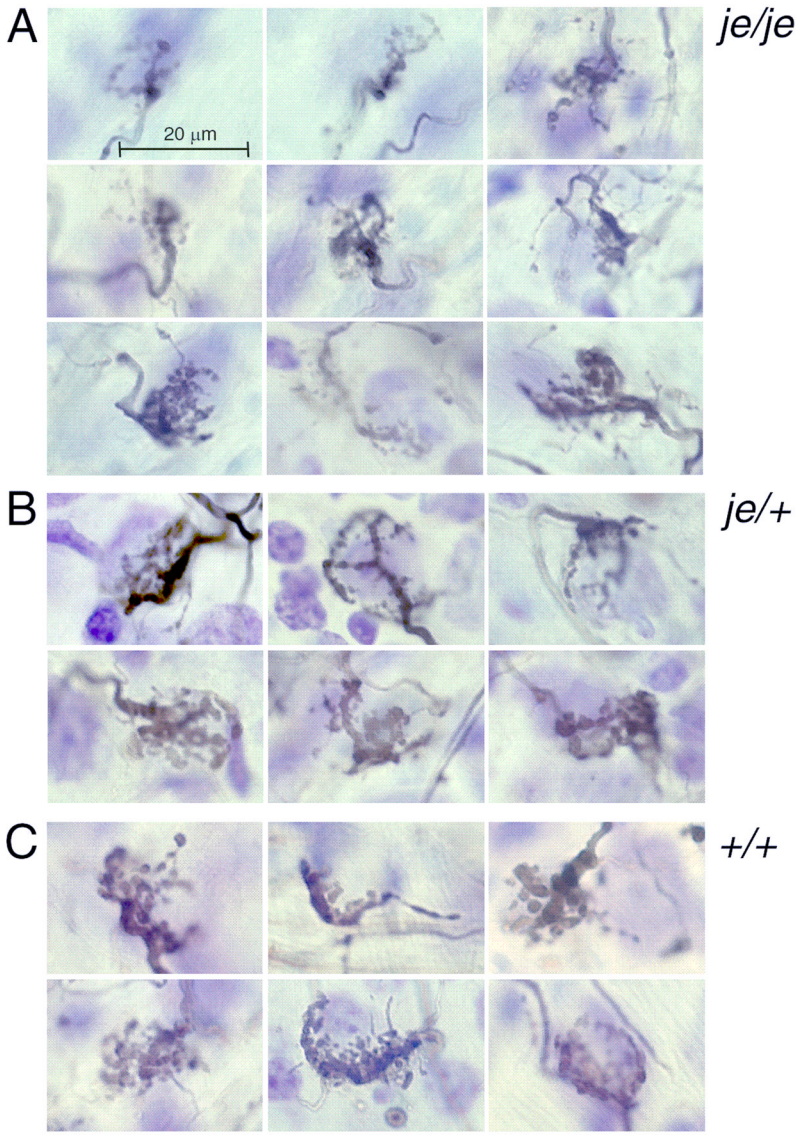

Figure 3.

Near and anterior to the nerve root auditory nerve fibers commonly terminate in large terminals, the end bulbs of Held. End bulbs were variable in size and shape in all mice but there seemed to be a subtle difference between end bulbs in *je*/*je* and in hearing heterozygote and wild type mice. End bulbs were selected for their size and for the resolution of their structure in photomicrographs. A. In *je*/*je* mice end bulbs tended to be smaller and comprised smaller, more filamentous processes than in hearing mice. B. In heterozygous *je*/+ mice, many end bulbs were larger and composed of larger terminal swellings than in the homozygotes. C. End bulbs in wild type animals were similar to those in heterozygotes. No differences were detected between the ICR and CBA strains of mice; the panels in the left column are from ICR mice, those in the middle and right columns from CBA mice.

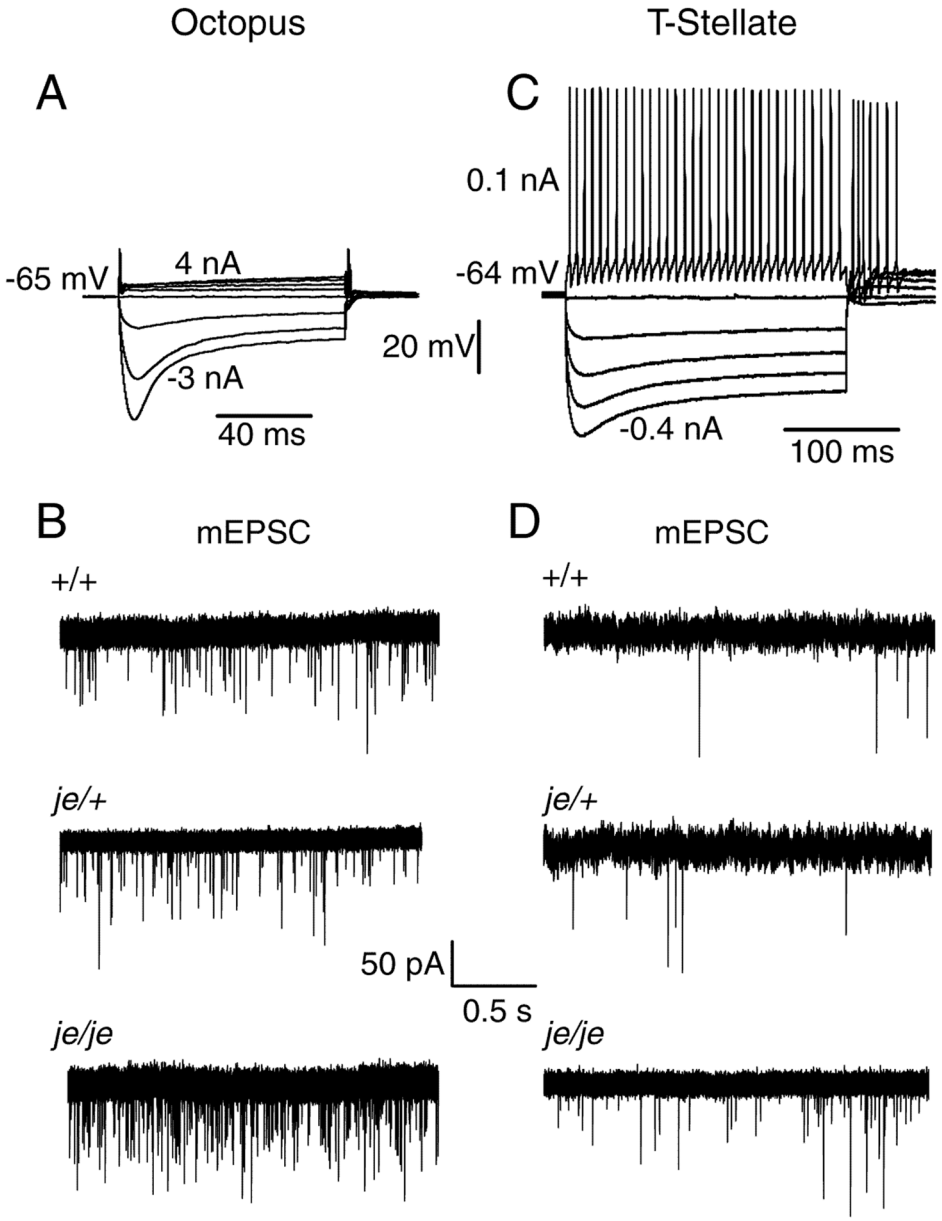

Figure 4.

Spontaneous miniature excitatory postsynaptic currents (mEPSC) are more frequent in octopus and T stellate cells of deaf *je*/*je* than of hearing *je*/+ or wild type mice. A: Responses to current pulses identify this to be an octopus cell in a slice from a +/+ ICR mouse. Large depolarizing currents were required to bring the cell to threshold. As is typical, this octopus cell fired only once at the onset of a suprathreshold depolarizing current pulse and at the offset of hyperpolarizing pulses. B: Representative traces show examples of mEPSCs from octopus cells of +/+, *je*/+ and *je*/*je* mice. Cells were held near their resting membrane potential at −65 mV. C: Responses to current pulses show that small current pulses bring the cell to threshold and that depolarization evokes a train of regular action potentials that identify it to be a T stellate cell in this recording from a +/+ ICR mouse. D: In T stellate cells the frequency of mEPSC is lower than in octopus cells. Each of the traces in B and D shows a single, continuous record.

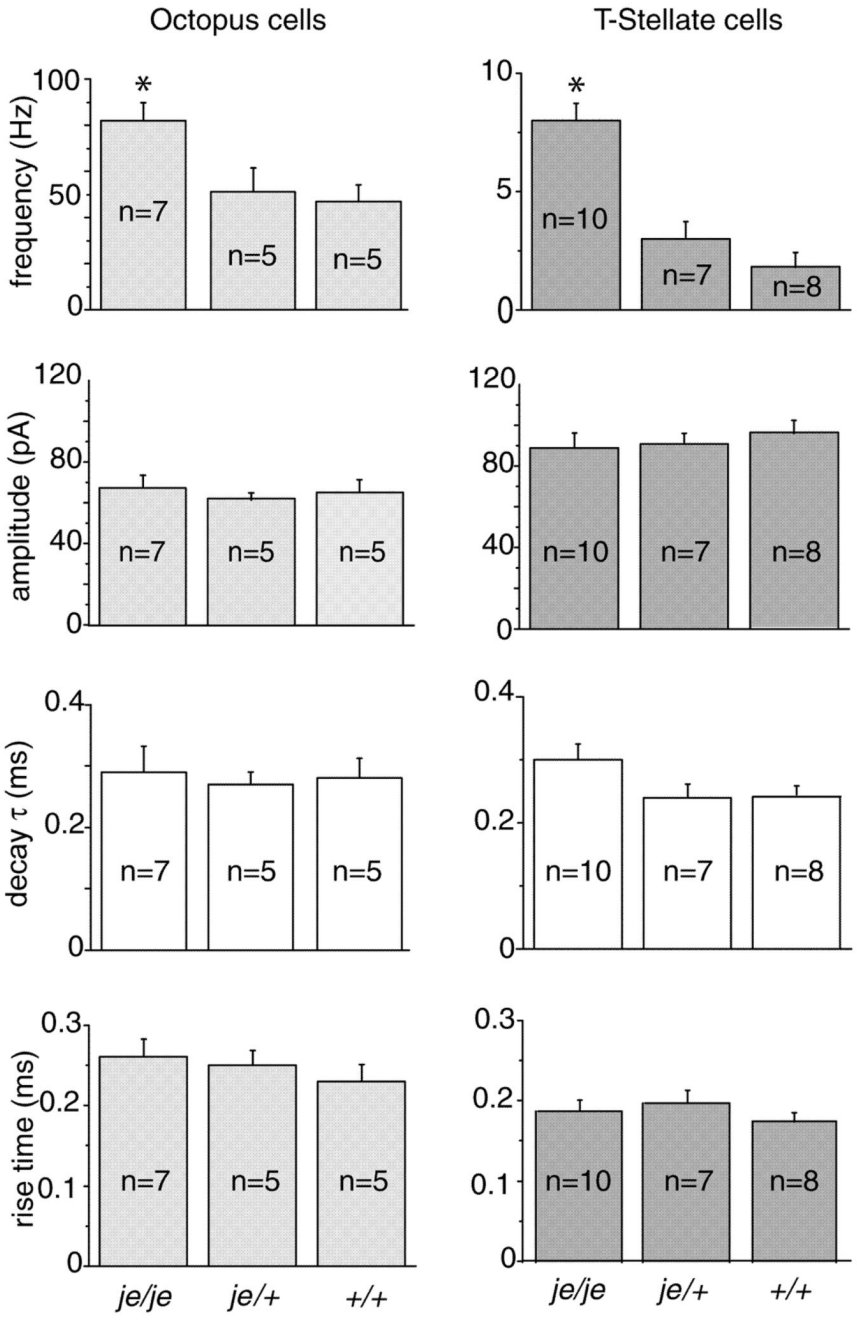

Figure 5.

Statistical effects of genotype and cell type were tested by means of a two-way ANOVA followed by Tukey's post test. These tests showed that the frequency of occurrence of mEPSCs is higher in deaf *je*/*je* than in hearing *je*/+ or +/+ mice; statistically significant differences between genotype are designated with asterisks (*). Octopus cells had more frequent mEPSCs but they were smaller and more slowly rising than those in T stellate cells; statistically significant differences between cell types are illustrated by differences in gray intensity.

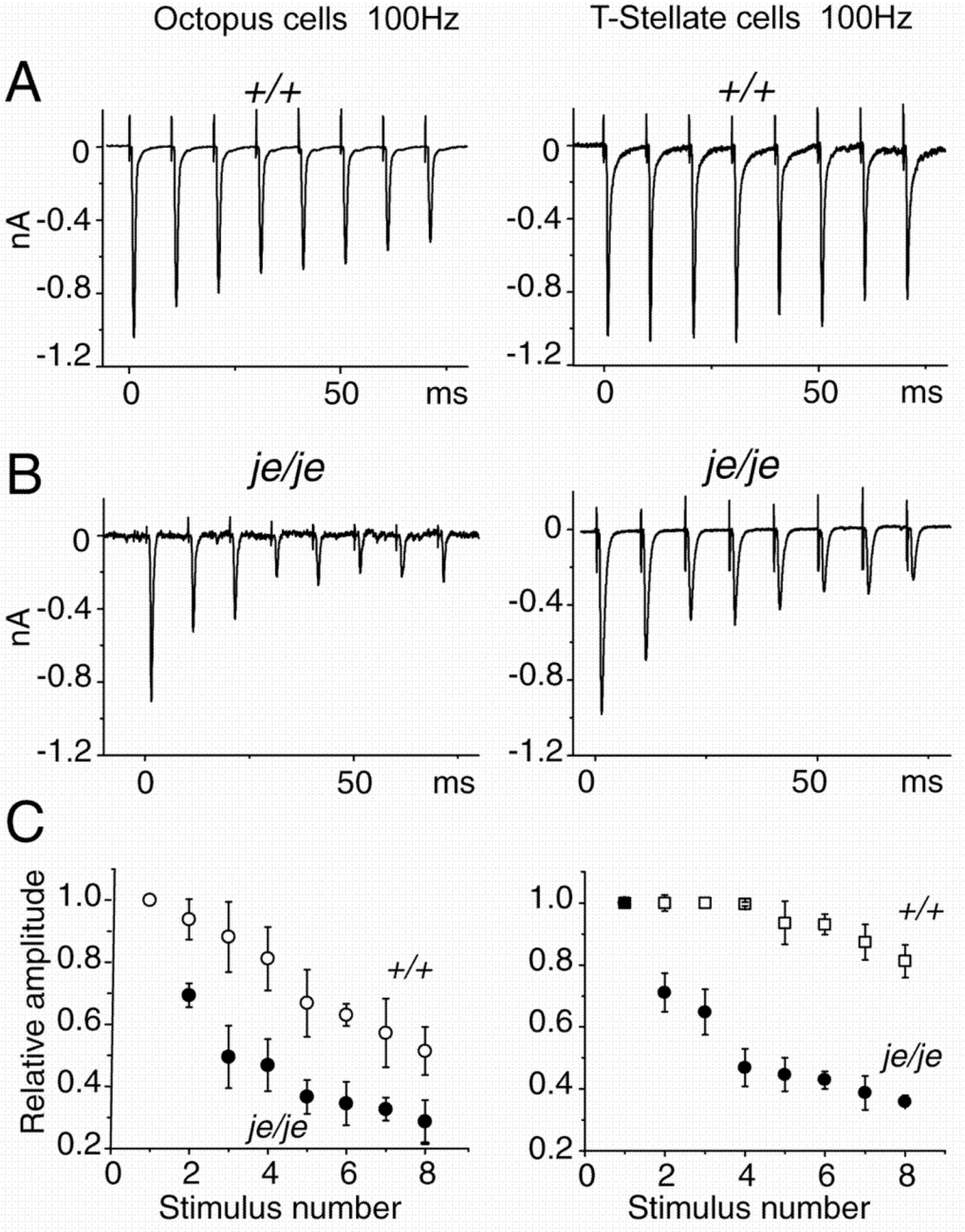

Figure 6.

Synaptic depression in responses to trains of shocks at 100 Hz is greater in *je*/*je* than in wild type mice. A. Averages of responses to 10 trains, with 30 sec between trains, were recorded from an octopus and a T-stellate cell of wild type mice as shown. Synaptic responses in octopus cells showed more depression than those in T stellate cells. B. In *je*/*je* mice responses to similar trains show more depression in both octopus and T stellate cells than in wild type mice, but depression remains greater in octopus than in T stellate cells. C. Depression during 100Hz trains was compared by normalizing each EPSC to the first EPSC of each train in octopus cells (left) and T-stellate cells (right). The pattern observed in individual cells is observed in the populations. Depression is significantly greater in both

cell types in *je*/*je* than in wild type mice for stimuli 2–8 of trains ($p<0.01$); depression is greater in octopus than in T stellate cells. Trains of stimuli were presented with 30 secs between trains. Responses to between 10 and 30 trains were averaged for each condition. Plots show averages from 6 *je*/*je* octopus cells, 5 +/+ octopus cells, 5 *je*/*je* T stellate cells and 5 +/+ T stellate cells.

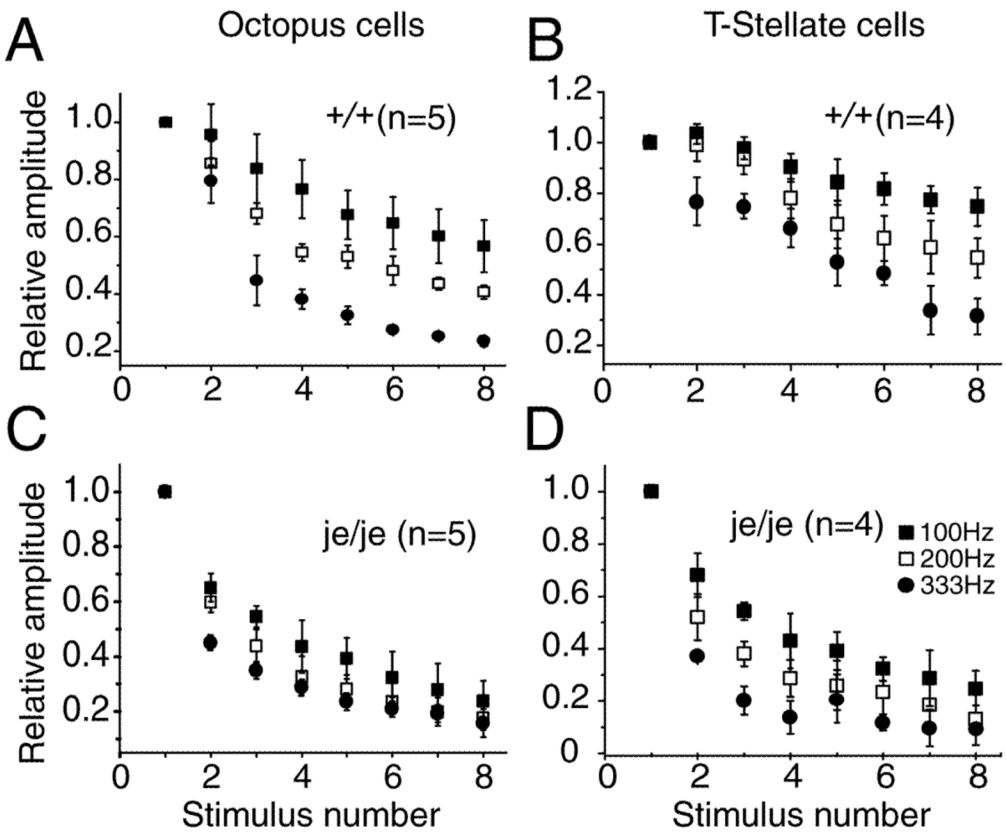

Figure 7.

Depression during trains of EPSCs depended on stimulation rate and was greater in *je*/*je* than in wild type mice. A. In octopus cells of wild type mice, depression increased with stimulation rate. B. In T stellate cells synaptic depression also increased with the rate at which the strains of stimuli were presented but at all frequencies, there was less depression than in octopus cells. C. In *je*/*je* animals depression in octopus cells was greater at 100 Hz and 200 Hz but at 333 Hz depression was similarly strong. D. In T stellate cells of *je*/*je* animals depression was greater than in +/+ mice at all stimulation rates.

Table 1

Numbers of slices and the age range of animals from which they were taken for electrophysiological measurements.

	P17–P18	P19–P20	P21–22
je/*je*		4	33
je/+	7	4	1
+/+	31	5	1

Table 2

Comparison of intrinsic electrical properties in wild type and *jerker* mice reveal no differences.

	+/+		*je*/*je*	
	Octopus (n=6)	**T stellate (n=8)**	**Octopus (n=4)**	**T stellate (n=5)**
V_{rest}, mV	−63.7 ± 5.1	−64.5 ± 4.2	−59.2 ± 4.3	−65.2 ± 5.3
$R_{in,}$ MΩ	7.3 ± 1.6	91.2 ± 11.4	8.1 ± 1.7	97.4 ± 14.2
τ, ms	0.3 ± 0.1	8.2 ± 1.7	0.4 ± 0.1	8.7 ± 1.6

Values of resting potential (V_{rest}), input resistance (R_{in}), and membrane time constant (τ) are given as means ± SE. The R_{in} and τ were measured near the resting potential.